DTU Library

Process conditions and volumetric composition in composites

Madsen, Bo

Published in:
Proceedings of the Risø International Symposium on Materials Science

Publication date:
2013

Document Version
Publisher's PDF, also known as Version of record

Link back to DTU Orbit

Citation (APA):
Madsen, B. (2013). Process conditions and volumetric composition in composites. Proceedings of the Risø International Symposium on Materials Science, 34, 37-54.

PROCESS CONDITIONS AND VOLUMETRIC COMPOSITION
IN COMPOSITES

Bo Madsen

Composites and Materials Mechanics, Department of Wind Energy,
Technical University of Denmark, Risø Campus,
DK-4000 Roskilde, Denmark

ABSTRACT

The obtainable volumetric composition in composites is linked to the gravimetric composition, and it is influenced by the conditions of the manufacturing process. A model for the volumetric composition is presented, where the volume fractions of fibers, matrix and porosity are calculated as a function of the fiber weight fraction, and where parameters are included for the composite microstructure, and the fiber assembly compaction behavior. Based on experimental data of composites manufactured with different process conditions, together with model predictions, different types of process related effects are analyzed. The applied consolidation pressure is found to have a marked effect on the volumetric composition. A power-law relationship is found to well describe the found relations between the maximum obtainable fiber volume fraction and the consolidation pressure. The degree of fiber/matrix compatibility and the related amount of interface porosity is found to have a negligible effect on the volumetric composition. Only for the extreme case where an interface gap of 250 nm is considered to exist along the entire fiber perimeter, the porosity of the composites is noticeable above zero, but still the fiber and matrix volume fractions are only slightly changed. Air entrapment in the matrix due to non-ideal process conditions is found to have a marked effect on the volumetric composition. For composites with such type of matrix porosity, the porosity content is decreased when the fiber content is increased. Altogether, the model is demonstrated to be a valuable tool for a quantitative analysis of the effect of process conditions. Based on the presented findings and considerations, examples of future work are mentioned for the further improvement of the model.

1.   INTRODUCTION

The volumetric composition in composites, their fiber, matrix and porosity content, is a fundamental characteristic for the materials performance. Micromechanical models are used to link the volumetric composition to the (mechanical) property profile of the composites. The obtainable volumetric composition of composites is however constrained by the applied

manufacturing concept, and furthermore, it is influenced by the setting of process conditions. Thus, the study of the relations between process conditions and volumetric composition in composites is central to the goal of achieving maximum materials performance.

Typically, prior to the manufacturing process, model equations for weight and volume relationships are used to convert the controlled gravimetric composition into a wanted volumetric composition. These calculations are simple if assumptions of no porosity and unlimited fiber packing ability are applied, but they become less simple for the realistic situation of composites with porosity and limited fiber packing ability. The latter situation requires however knowledge on the composite microstructure, and the compaction behavior of the fiber assembly. These parameters are included in a model for the volumetric composition in composites developed by Madsen, Thygesen and Lilholt (2007), which later on was integrated in a micromechanical model for stiffness of composites (Madsen, Thygesen and Lilholt 2009). The model has recently been used in the studies by Aslan, Mehmood and Madsen (2013) and Domínguez and Madsen (2013).

The objective of the present study is to use the volumetric composition model for a quantitative analysis of the effect of process conditions on the volumetric composition in composites. Initially, the basic definitions of gravimetric and volumetric composition in composites are presented, followed by a presentation of model concepts and key equations. Based on experimental data of composites manufactured with different process conditions, together with model predictions, three types of process related effects are analyzed: (i) *consolidation pressure*, which is a typical variable process condition, (ii) *fiber/matrix compatibility*, which is governed by e.g. the surface polarity of the two parts, and (iii) *air entrapment in matrix*, which is due to e.g. generation of volatile by-products during curing of a thermosetting resin matrix.

2. BASIC DEFINITIONS

Composite materials are typically composed of two materials parts, fibers and matrix, together with a third part, porosity, which consists of air-filled cavities within the composites. The three parts in composites are schematically illustrated in Fig. 1 showing them in their intermixed configuration (left) or visualized as discrete slabs on top of each other (right).
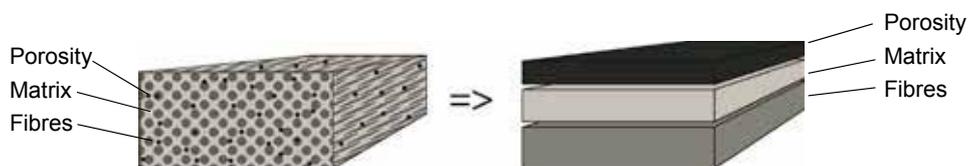

Fig. 1. Schematic illustration of the three parts in composites, fibers, matrix and porosity.

On a weight basis, composites consist of fibers and matrix, and their weight fractions sum to one:

$$m_c = m_f + m_m \quad \Rightarrow \quad 1 = \frac{m_f}{m_c} + \frac{m_m}{m_c} = W_f + W_m \quad (1)$$

where m is absolute mass, W is weight fraction, and the subscripts c, f and m are composite, fibers, and matrix, respectively.

On a volume basis, composites consist of fibers, matrix and porosity, and their volume fractions sum to one:

$$v_c = v_f + v_m + v_p \quad \Rightarrow \quad 1 = \frac{v_f}{v_c} + \frac{v_m}{v_c} + \frac{v_p}{v_c} = V_f + V_m + V_p \quad (2)$$

where v is absolute volume, V is volume fraction, and the subscript p is porosity.

Accordingly, composites are characterized by having (i) a *gravimetric composition* (W_f and W_m), which typically can be directly controlled by the ingoing masses of fibers and matrix in the manufacturing process, and (ii) a *volumetric composition* (V_f, V_m and V_p), which is influenced by the process conditions of the manufacturing process.

3. MODELS FOR VOLUMETRIC COMPOSITION

Equations for the weight/volume relations in composites are required to convert between the controllable weight fractions and the resulting volume fractions, where the latter ones govern the mechanical properties of the composites. Here follow presentations of two models for volumetric composition in composites.

3.1 Traditional model for volumetric composition. For the case of composites with *no porosity* ($V_p = 0$) and *unlimited fiber packing ability* ($V_f \in [0; 1]$), the governing equations can readily be derived:

$$V_{f*} = \frac{v_f}{v_f + v_m} = \frac{\dfrac{m_f}{\rho_f}}{\dfrac{m_f}{\rho_f} + \dfrac{m_m}{\rho_m}} = \frac{W_f \, \rho_m}{W_f \, \rho_m + \left(1 - W_f\right) \rho_f}$$

$$V_{m*} = \frac{v_m}{v_f + v_m} = \frac{\dfrac{m_m}{\rho_m}}{\dfrac{m_f}{\rho_f} + \dfrac{m_m}{\rho_m}} = \frac{\left(1 - W_f\right)\rho_f}{W_f \, \rho_m + \left(1 - W_f\right)\rho_f} = 1 - V_{f*} \quad (3, 4, 5)$$

$$V_{p*} = 1 - (V_{f*} + V_{m*}) = 0$$

where ρ_f and ρ_m are density of fibers and matrix, respectively. The asterisk (*) specifies the situation of no porosity and unlimited fiber packing ability. These are the equations traditionally shown in text books of composites.

3.2 New model for volumetric composition. In the more realistic case of composites *with porosity* ($V_p > 0$) and *limited fiber packing ability* ($V_f \in [0; V_{f\,max}]$ where $V_{f\,max} < 1$), a model has been developed by Madsen et al. (2007).

The model predicts two regions of composite volumetric composition: Region A and B, which are separated by a transition point. Fig. 2 shows an example of predicted volume fractions of fibers, matrix and porosity as a function of the fiber weight fraction. The figure shows also schematized cross-sections of composites.

In Region A, where the fiber weight fraction is below a transition value, $W_{f\,trans}$, the fiber assembly is *not fully compacted* (under the operating process conditions), and the volume of matrix is *sufficient* to fill the free space between the fibers (see schematized composite cross-sections in Fig. 2). In this situation, the volumetric composition (V_f, V_m and V_p) is governed by the equations:

$$V_f = \frac{W_f \, \rho_m}{W_f \, \rho_m \left(1 + \sum \alpha_{pf\,(i)}\right) + \left(1 - W_f\right) \, \rho_f \left(1 + \sum \alpha_{pm\,(i)}\right)}$$

$$V_m = \frac{\left(1 - W_f\right) \rho_f}{W_f \, \rho_m \left(1 + \sum \alpha_{pf\,(i)}\right) + \left(1 - W_f\right) \, \rho_f \left(1 + \sum \alpha_{pm\,(i)}\right)} \quad (6, 7, 8)$$

$$V_p = 1 - \left(V_f + V_m\right)$$

where $\alpha_{pf\,(i)}$ and $\alpha_{pm\,(i)}$ are so-called fiber and matrix correlated porosity factors, respectively, which control the porosity content in the composites (see Section 3.3). It can be noted that if the porosity factors are set equal to zero, then Eqs. (6) - (8) become identical to Eqs. (3) - (5) representing the simple case of no porosity.

In Region B, where the fiber weight fraction is above the transition value, $W_{f\,trans}$, the fiber assembly is *fully compacted* (under the operating process conditions), and the volume of matrix is *insufficient* to fill the free space between the fibers (see schematized composite cross-sections in Fig. 2). Since the fiber assembly is fully compacted to its minimum volume, it means that the volumetric composition is constrained by a maximum obtainable fiber volume fraction, $V_{f\,max}$. In this situation, the volumetric composition (V_f, V_m and V_p) is governed by the equations:

$$V_f = V_{f\,max}$$

$$V_m = V_{f\,max} \frac{\left(1 - W_f\right) \rho_f}{W_f \, \rho_m} \quad (9, 10, 11)$$

$$V_p = 1 - \left(V_f + V_m\right)$$

The transition point between Region A and B, as defined by $W_{f\,trans}$, can be calculated by the equation:

$$W_{f\,trans} = \frac{V_{f\,max} \, \rho_f \left(1 + \sum \alpha_{pm\,(i)}\right)}{V_{f\,max} \, \rho_f \left(1 + \sum \alpha_{pm\,(i)}\right) - V_{f\,max} \, \rho_m \left(1 + \sum \alpha_{pf\,(i)}\right) + \rho_m} \quad (12)$$
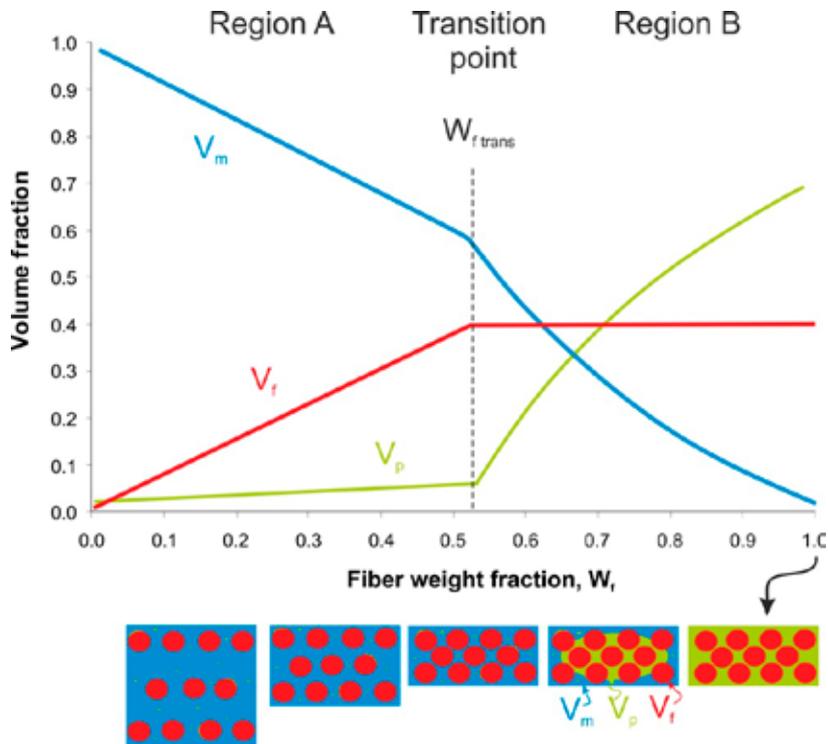
Fig. 2. Model diagram of the volumetric composition (V_f, V_m and V_p) in composites as a function of the fiber weight fraction (W_f), together with schematized composite cross sections. Color codes: red for fibers, blue for matrix, and green for porosity. (Aslan et al. 2013).

As shown in Fig. 2, at the transition point between Region A and B, the volumetric composition is characterized by the best possibly combination of high V_f and low V_p, and this typically results in composites with maximum mechanical properties (Madsen et al. 2009; Aslan et al. 2013). This is exemplified in Fig. 3 for unidirectional flax fiber/polyethylene terephthalate composites showing both the volumetric composition, and the stiffness of the composites as a function of the fiber weight fraction. The model lines predict a transition fiber weight fraction of 0.61, at which V_f is 0.53 and V_p is 0.07, and this corresponds to a maximum obtainable stiffness of the composites on 35 GPa. Thus, it is demonstrated that the transition point is valuable at giving the optimum parameters for composite design.

In general, as shown in Fig. 3, and as will be shown later, there is a good agreement between experimental data and predictions made by the developed new model for volumetric composition in composites.
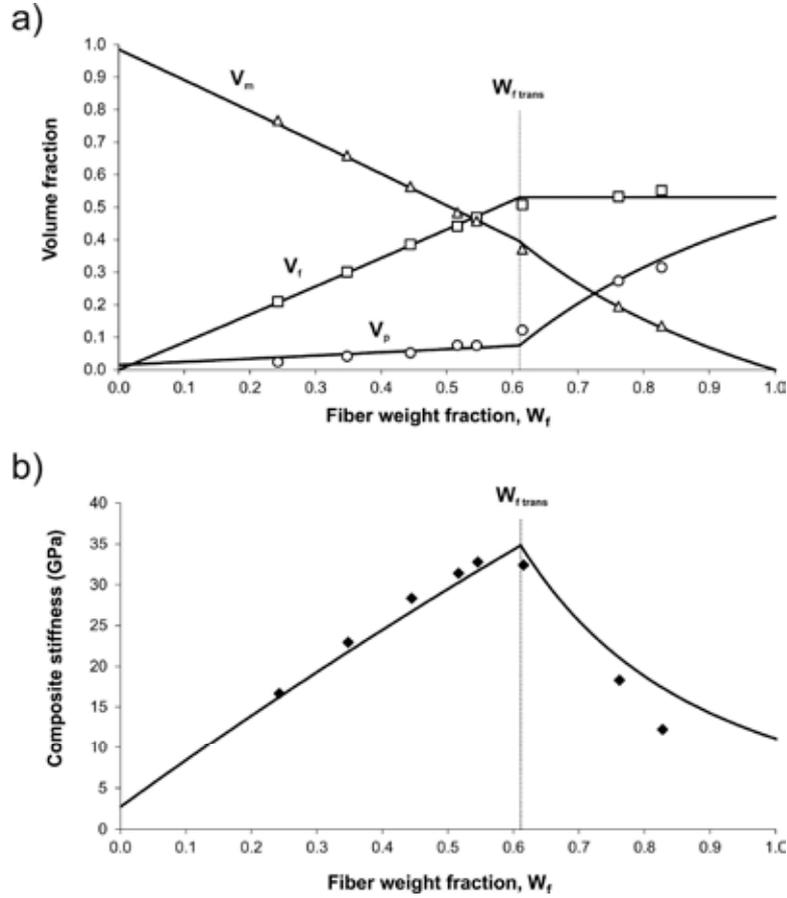
Fig. 3. Experimental data and model predictions of (a) volumetric composition (V_f, V_m and V_p) and (b) stiffness as a function of the fiber weight fraction (W_f) of unidirectional flax fiber/ polyethylene terephthalate composites. Experimental data from Aslan et al. (2013).

3.3 Identification and quantification of porosity types. In the above presented model for volumetric composition in composites, the total porosity (V_p) can be divided into a number of different types of porosity:

$$V_p = \sum V_{pf\,(i)} + \sum V_{pm\,(i)} + V_{ps} \tag{13}$$

where $V_{pf\,(i)}$ are different types of *fiber correlated porosity*, $V_{pm\,(i)}$ are different types of *matrix correlated porosity*, and V_{ps} is *structural porosity*.

The fiber and matrix correlated porosity fractions ($V_{pf\,(i)}$ and $V_{pm\,(i)}$) are assumed to be linearly related to the fiber and matrix volume fractions (V_f and V_m) via the *fiber and matrix correlated porosity factors* ($\alpha_{pf\,(i)}$ and $\alpha_{pm\,(i)}$), respectively:

$$\sum V_{pf\,(i)} = \sum \alpha_{pf\,(i)}\, V_f \qquad ; \qquad \sum V_{pm\,(i)} = \sum \alpha_{pm\,(i)}\, V_m \tag{14, 15}$$

The porosity factors $\alpha_{pf\,(i)}$ and $\alpha_{pm\,(i)}$ are parameters in the volumetric composition model (see Eqs. (6) and (7)).

Three different types of fiber correlated porosities have been identified:
- Fiber porosity ($V_{pf\,(1)}$), which is identified as air-filled cavities inside the fibers, i.e. fibers with a so-called lumen.
- Interface porosity ($V_{pf\,(2)}$), which is identified as air-filled cavities (gaps) at the fiber/matrix interface.
- Impregnation porosity ($V_{pf\,(3)}$), which is identified as air-filled cavities in the interior of fiber sub-assemblies (e.g. fiber bundles).

One type of fiber correlated porosity has been identified:
- Matrix porosity ($V_{pm\,(1)}$), which is identified as air-filled cavities in the matrix (e.g. entrapped air bubbles).

As indicated by Eqs. (14) and (15), each of the above-mentioned four types of porosities ($V_{pf\,(1)}$, $V_{pf\,(2)}$, $V_{pf\,(3)}$, and $V_{pm\,(1)}$) is assigned a porosity factor ($\alpha_{pf\,(1)}$, $\alpha_{pf\,(2)}$, $\alpha_{pf\,(3)}$, and $\alpha_{pm\,(1)}$). In the study by Madsen et al. (2007), analytical equations were derived to determine three out of four porosity factors:

$$\alpha_{pf\,(1)} = \frac{V_{lumen}}{1 - V_{lumen}} \qquad \text{i.e.} \qquad V_{pf\,(1)} = \alpha_{pf\,(1)}\ V_f$$

$$\alpha_{pf\,(2)} = \frac{b\,\beta\,C}{A}\,\frac{1}{1 - V_{lumen}} \qquad \text{i.e.} \qquad V_{pf\,(2)} = \alpha_{pf\,(2)}\ V_f \qquad\qquad (16,\ 17,\ 18)$$

$$\alpha_{pm\,(1)} = \frac{V_{matrix\ porosity}}{1 - V_{matrix\ porosity}} \qquad \text{i.e.} \qquad V_{pm\,(1)} = \alpha_{pm\,(1)}\ V_m$$

where V_{lumen} is the volume fraction of lumen in the fibers, b is the width of the interface gap, β is the interface debonding fraction of the fiber perimeter ($\beta = 1$ for fully debonded fibers), A is the cross-sectional area of the fibers, C is the perimeter of the fiber cross-section, and $V_{matrix\ porosity}$ is the volume fraction of porosity in the matrix. It should be noted that each of these parameters are physically meaningful, and they can in principle be directly measured from the microstructure of composites.

An analytical equation has however not been derived for the impregnation porosity factor ($\alpha_{pf\,(3)}$). Instead, the value of this porosity factor can be found from the slope of a linear regression line of the relation between experimental data of total porosity (V_p) and fiber volume fraction (V_f) for composites with variable fiber content (for data in Region A of the model), and by knowledge of the values of the other three porosity factors:

$$V_p = \frac{\alpha_{pf\,(1)} + \alpha_{pf\,(2)} + \alpha_{pf\,(3)} - \alpha_{pm\,(1)}}{1 + \alpha_{pm\,(1)}}\ V_f + \frac{\alpha_{pm\,(1)}}{1 + \alpha_{pm\,(1)}} \qquad (19)$$

Structural porosity (V_{ps}), the final part of the total porosity (see Eq. (13)), is formed due to the situation in Region B where the available matrix volume is insufficient to fill the free space in the fully compacted fiber assembly. This type of porosity is responsible for the considerable increase of the total porosity in Region B as shown in Figs. 2 and 3.

4.   PROCESS CONDITIONS AND VOLUMETRIC COMPOSITION

Based on experimental data and model predictions, here follows an analysis of three types of process related effects on the volumetric composition in composites.

4.1 Effect of consolidation pressure. The applied pressure used to consolidate composite materials during manufacturing is the key important process condition used to control the resulting fiber volume fraction. Furthermore, the consolidation pressure can also be linked to the porosity content of the composites. In general, it can be expected that the higher the applied consolidation pressure, the higher the resulting fiber volume fraction, and the lower the resulting porosity content. These expected relations will be quantitatively analyzed.

In previous studies of different types of composites, series of composite plates have been manufactured with variable consolidation pressures:
- 2D random oriented flax/polypropylene composites, autoclave consolidation with pressures of 0.7 and 2.1 MPa (Toftegaard 2002; Madsen et al. 2007).
- Unidirectional flax/polyethylene terephthalate composites, press consolidation with pressures of 1.7 and 4.2 MPa (Aslan et al. 2013).
- Biaxial (± 45°) flax/epoxy composites, vacuum and autoclave consolidation with pressures of 0.1 and 0.8 MPa (Markussen, Prabharakan, Toftegaard and Madsen 2013).
- Biaxial (± 45°) glass/epoxy composites, vacuum and autoclave consolidation with pressures of 0.1 and 0.8 MPa (Markussen et al. 2013).

The experimental data of volumetric composition as function of the fiber weight fraction for the composites are shown in Figs. 4, 5, 6 and 7. Shown are also the predicted volumetric compositions using the above presented model. For means of simplicity, and to make the analysis easier to comprehend, only the results for V_f and V_p are shown in the figures. The results of the complimentary matrix volume fraction ($V_m = 1 - V_f - V_p$) are not shown. The determined model parameters used for the predictions are shown in Table 1.

For the 2D random oriented flax/PP composites (Fig. 4), there is a clear effect of the increased consolidation pressure from 0.7 to 2.1 MPa. The maximum obtainable fiber volume fraction ($V_{f\ max}$) is increased from 0.33 to 0.41, which corresponds to an increase of the transition fiber weight fraction ($W_{f\ trans}$) from 0.52 to 0.58. In the study by Madsen et al. (2009), it is reported that the corresponding maximum stiffness of the composites at $W_{f\ trans}$ is 5.8 and 6.3 GPa, respectively. In Fig. 4, it can also be observed that in Region A (for W_f below $W_{f\ trans}$), the porosity of the composites is markedly reduced when the consolidation pressure is increased, and this is quantitatively described by a decrease of the impregnation porosity factor from 0.41 to 0.19 (see Table 1). Thus, the higher pressure leads to a more efficient impregnation of the flax fiber bundles by the PP matrix.

For the unidirectional flax/PET composites (Fig. 5), the effect of the increased consolidation pressure from 1.7 to 4.2 MPa is to increase $V_{f\ max}$ from 0.53 to 0.60, which corresponds to an increase of $W_{f\ trans}$ from 0.61 to 0.68. In addition, the impregnation porosity factor is decreased from 0.12 to 0.09. Thus, these changes are comparable to the ones for the flax/PP composites, although the flax/PET composites show a relatively smaller decrease of the impregnation porosity which can be due to the already low porosity content of the low pressure composites. At $W_{f\ trans}$, the maximum stiffness of the low and high pressure composites have been reported to be 35 and 40 GPa, respectively (Aslan et al. 2013) (see also Fig. 3b).

Process conditions and volumetric composition in composites

Table 1. Determined model parameters for different types of experimental composite materials manufactured with different techniques. PET is polyethylene terephthalate, PP is polypropylene, and FA is polyfurfuryl alcohol.

	Type of composites								
	Flax/PP		**Flax/PET**		**Flax/epoxy**		**Glass/epoxy**		**Glass/FA**
Fiber orientation	2D random		Unidirectional		Biaxial ($\pm 45°$)		Biaxial ($\pm 45°$)		Biaxial ($\pm 45°$)
Fiber/matrix mixing technique	Film-stacking		Filament-winding		Vacuum infusion		Vacuum infusion		Hand-layup
Consolidation technique	Autoclave		Press		Vacuum and autoclave		Vacuum and autoclave		Vacuum
Consolidation pressure [MPa]	0.7	2.1	1.7	4.2	0.1	0.8	0.1	0.8	0.1
Maximum fiber volume fraction, $V_{f\,max}$	0.33	0.41	0.53	0.60	0.28	0.38	0.51	0.64	0.51[a]
Transition fiber weight fraction, $W_{f\,trans}$	0.52	0.58	0.61	0.68	0.33	0.45	0.70	0.80	0.69
Impregnation porosity factor, $\alpha_{pf(3)}$	0.41	0.19	0.12	0.09	0		0		0
Interface porosity factor, $\alpha_{pf(2)}$	0.01		0.01		0		0		0
Fiber porosity factor, $\alpha_{pf(1)}$	0.03		0.01		0.01		0		0
Matrix porosity factor, $\alpha_{pm(1)}$	0		0.01		0.01		0		0.10
Fiber density, ρ_f [g/cm^3]	1.54		1.59		1.52		2.60		2.62
Matrix density, ρ_m [g/cm^3]	0.91		1.36		1.15		1.15		1.36
Reference	Toftegaard 2002; Madsen et al. 2007		Aslan et al. 2013		Markussen et al. 2013		Markussen et al. 2013		Domínguez and Madsen 2013

[a] Assumed value based on the determined value for the related glass/epoxy composite.

The above presented two types of flax fiber composites are manufactured by an initial mixing of fibers and matrix by *film-stacking* or *filament-winding*, followed by consolidation of the fiber/matrix assembly by autoclave or press. These manufacturing techniques give a direct way of varying the consolidation pressure to control the volumetric composition in the composites. In contrast, this is not readily possible for the biaxial flax/epoxy and glass/epoxy composites manufactured by the *vacuum infusion* technique. In this technique, the fiber assembly is initially compacted to the consolidation level by a vacuum bag, and then the fibers are impregnated by the infused matrix. Accordingly, by using the previously used terminology for the model, composites manufactured by vacuum infusion will be exactly at the transition point where the fiber assembly is *fully compacted*, and the volume of matrix is *just sufficient* to fill the free space between the fibers, and consequently, W_f equals $W_{f\,trans}$, and V_f equals $V_{f\,max}$. Thus, for the given operating process conditions, in particular the applied vacuum pressure, the vacuum infusion technique inevitably gives composites with the best possible combination of high fiber volume fraction and low porosity content, leading to the best possible properties. This is the advantage of the vacuum infusion technique, whereas the disadvantage is the involved practical difficulties to further improve the volumetric composition, i.e. to increase the fiber volume fraction above the (rather low) value given by the vacuum pressure.
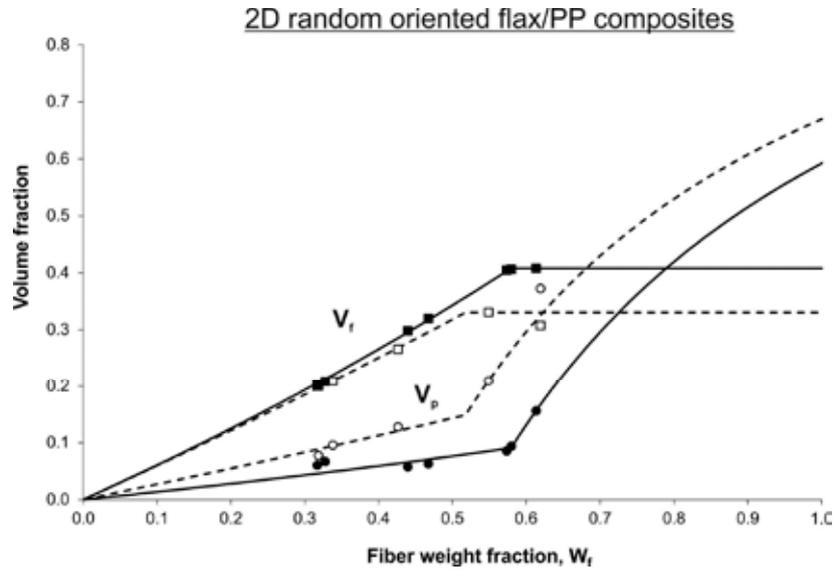
Fig. 4. Experimental data and model predictions of the volumetric composition in 2D random oriented flax/polypropylene (PP) composites manufactured by film-stacking and autoclave consolidation with low and high pressures: 0.7 MPa (open symbols, dotted lines) and 2.1 MPa (filled symbols, full lines).
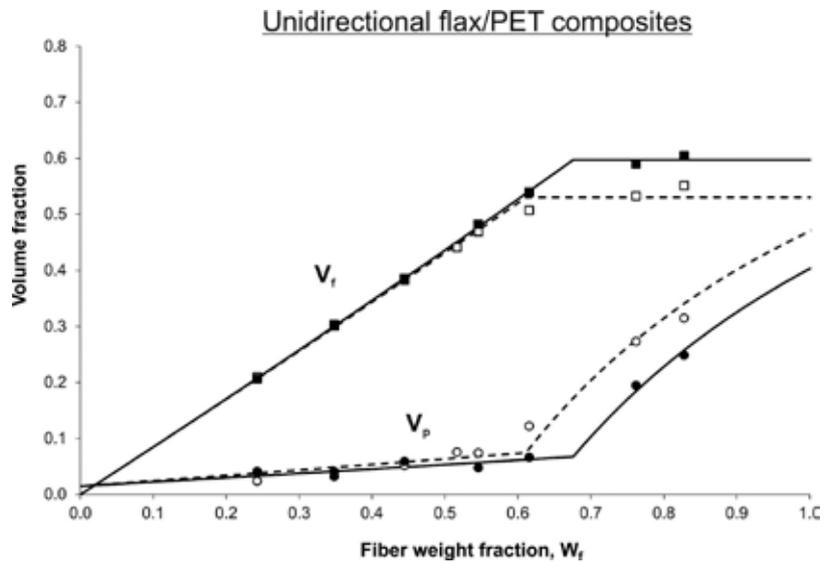

Fig. 5. Experimental data and model predictions of the volumetric composition in unidirectional flax/polyethylene terephthalate (PET) composites manufactured by filament-winding and press consolidation with low and high pressures: 1.7 MPa (open symbols, dotted lines) and 4.2 MPa (filled symbols, full lines). The results for the low pressure composites are also shown in Fig. 3.
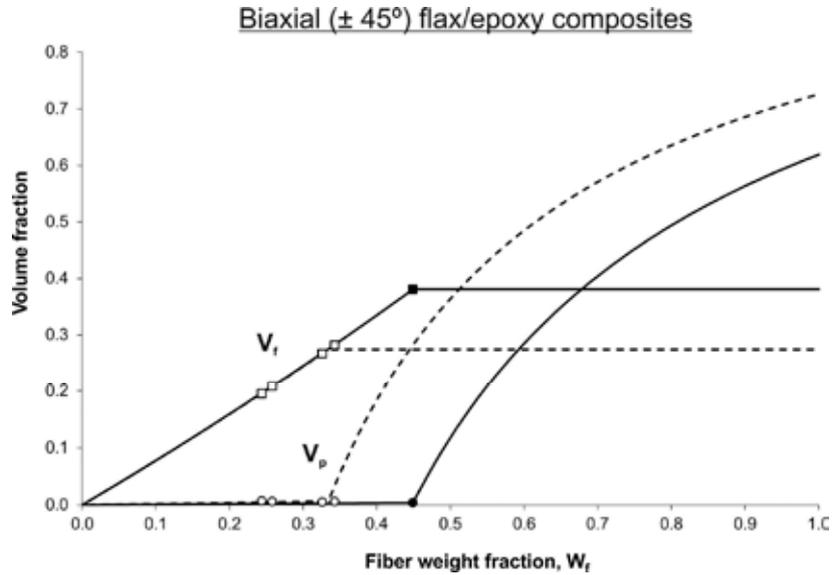
Fig. 6. Experimental data and model predictions of the volumetric composition in biaxial (± 45°) flax/epoxy composites manufactured by vacuum infusion with low and high consolidation pressures: 0.1 MPa (open symbols, dotted lines) and 0.8 MPa (filled symbols, full lines).

Fig. 7. Experimental data and model predictions of the volumetric composition in biaxial (± 45°) glass/epoxy composites manufactured by vacuum infusion with low and high consolidation pressures: 0.1 MPa (open symbols, dotted lines) and 0.8 MPa (filled symbols, full lines).
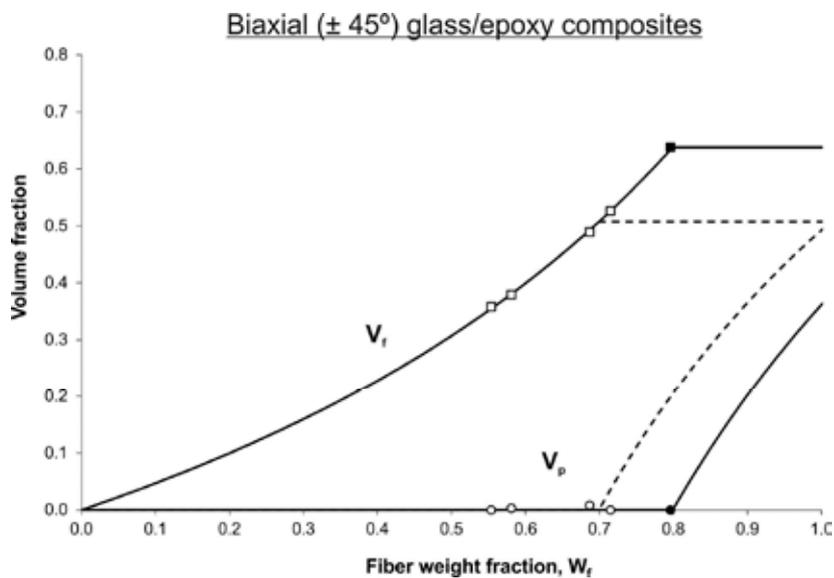
In the study by Markussen et al. (2013) of the biaxial flax/epoxy and glass/epoxy composites, the vacuum infusion technique was specially adapted to give composites with a different volumetric composition than the one normally given by the vacuum pressure. Composites were manufactured with (i) a lower V_f than $V_{f\,max}$ by enforcing an additional amount of matrix to the vacuum bag, and (ii) with a higher V_f than $V_{f\,max}$ by applying an additional external pressure on top of the vacuum pressure. The experimental data for the composites are shown in Figs. 6 and 7. The two groups of data points for low pressure are for composites consolidated by vacuum pressure (= 0.1 MPa), and the one data point for high pressure is for a composite consolidated by vacuum and external pressure (= 0.1 + 0.7 MPa). For both flax/epoxy and glass/epoxy composites, the low and high pressure model curves for V_f in Region A coincide, which means that if the fiber volume fraction is lowered below the value at the transition point (i.e. by enforcing an additional amount of matrix to the vacuum bag), then V_f will follow the same curve independently of the applied consolidation pressure. The increase of the consolidation pressure from 0.1 to 0.8 MPa however clearly results in an increase of V_f at the transition point (= $V_{f\,max}$) from 0.28 to 0.38 for the flax/epoxy composites, and from 0.51 to 0.64 for the glass/epoxy composites.

It can be expected that the relation between the consolidation pressure and the maximum obtainable fiber volume fraction in composites is governed by the compaction behavior of the fibers. In the literature, several studies have addressed the development of suitable models for compaction of fiber assembles (e.g. see Gutowski, Cai, Bauer, Boucher, Kingery and Wineman 1987; Simácek and Karbhari 1996; Toll 1998; Lomov and Verpoest 2000; Beil and Roberts 2002). Many of these are based on a power-law relationship:

$$V_f = a\, P^b \tag{20}$$

where P is the compaction pressure (MPa), and a and b are constants that can be related to the configuration of the fiber assembly (e.g. orientation and length of fibers), and the mechanical properties of the fibers (e.g. stiffness).

Fig. 8 presents the determined values of $V_{f\,max}$ as function of the consolidation pressure for the four types of composites (2D random flax/PP, UD flax/PET, biaxial flax/epoxy, and biaxial flax/epoxy). For each composite, a power-law relationship (Eq. (20)) has been fitted to the experimental data points. It can be observed that the curves are resembling the typical compaction curves measured for "dry" fiber assemblies, and moreover, they demonstrate the typical observed trend that (i) the packing ability is higher for glass fibers than for flax fibers (for assemblies with the same fiber orientation), and (ii) the packing ability is reduced when the fiber orientation is lowered (i.e. from unidirectional fibers to 2D randomly oriented fibers) (Madsen and Lilholt 2002).

For 2D random oriented fiber assemblies, it has been shown in theoretical studies by e.g. Toll and Manson (1995) and Toll (1998), based on geometrical and micromechanical considerations, that the exponent b in the power-law model will have a value of 1/5 (= 0.20). For unidirectional fiber assemblies, the exponent b cannot readily be determined analytically, but it has been evaluated from experimental data to be in the range 0.05 to 0.15 (Toll 1998; Madsen and Lilholt 2002). It can be observed in Fig. 8 that these theoretical values of b actually are close to the values estimated in the present study. For the biaxial glass fiber composite, which basically consists of unidirectional fiber assemblies on top of each other, the value of b is 0.11. For the unidirectional flax fiber composite, and the biaxial flax fiber composite, the value of b is about 0.15. The larger value of b for the flax fiber composites made from unidirectional fiber assemblies might be due to the twisted configuration of the flax fibers in the yarns, which means

that the fiber orientation deviates from being fully unidirectional. For the 2D random flax fiber composite, the value of b is 0.20, which is equal to the expected analytically determined value. However, in other experimental studies (Madsen and Lilholt 2002), the value of b for 2D random oriented fiber assemblies has been found to vary in the range 0.18 to 0.32. Based on observations of cross-sections of fiber assemblies, it has been indicated that the fiber dispersion (from single separated fibers to large fiber bundles) plays an important role for the measured variation in compaction behavior of 2D randomly oriented fiber assemblies (Madsen and Lilholt 2002).

Further to the above considerations of the compaction behavior of "dry" fiber assemblies, the compaction behavior of fiber assemblies during the composite consolidation process includes new parameters to be taken into account, such as the viscosity of the matrix, the lubrication of the fibers by the matrix, the elevated temperature, and the sustained pressure (creep). These parameters need to be included in the future goal of establishment of a model to relate the consolidation pressure with the maximum obtainable fiber volume fraction in composites.
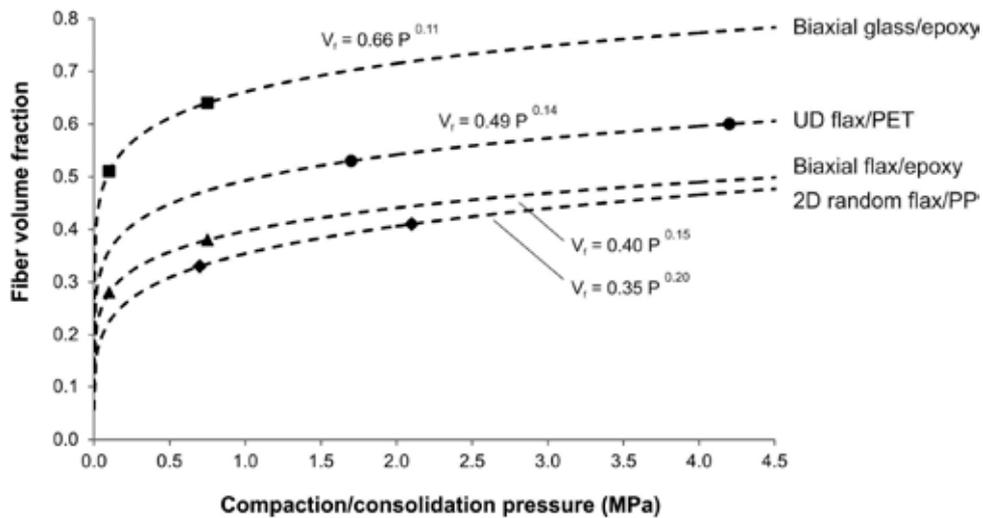

Fig. 8. Experimental data for the maximum obtainable fiber volume fraction, $V_{f\,max}$, as function of the consolidation pressure for different types of composites, together with fitted model curves (power-law relationships) for the compaction behavior of the fiber assemblies.

4.2 Effect of fiber/matrix compatibility. The compatibility between the fiber and matrix parts controls how closely the two parts can be contacted by each other in the composites. This is mainly governed by the surface polarity of the two parts. In the case of perfect fiber/matrix compatibility, intimate contact (< 1 nm) can be established between the two parts and chemical bonds (covalent, hydrogen, ionic or van der Waals) can be generated. This is the basis for obtaining a strong fiber/matrix interface bonding, which typically is considered to be essential for obtaining good mechanical properties of the composites. On the other hand, in the case of non-perfect fiber/matrix compatibility, intimate contact between the fiber and matrix parts cannot be established, and this can lead to air-filled cavities at the fiber/matrix interface regions. This so-called interface porosity can be formed both during processing of the composites, and during service of the materials due to external mechanical influences. In both cases, interface

49

porosity can be related to the degree of fiber/matrix compatibility.

The above presented model of volumetric composition contains parameters for quantifying the content of interface porosity in composites. In Eq. (17), the interface porosity factor ($\alpha_{pf\,(2)}$) is related to the width of the gap at the fiber/matrix interface (b), and the interface debonding fraction of the fiber perimeter (β) (where $\beta=1$ defines fully debonded fibers), in addition to parameters for the cross-sectional dimensions of the fibers. Fig. 9 shows examples of model predictions of the volumetric composition in glass fiber/epoxy composites with three realistic levels of interface porosity:

- No interface porosity, $\alpha_{pf\,(2)} = 0$ ($\beta = 0$; b = 250 nm).
- Medium interface porosity, $\alpha_{pf\,(2)} = 0.033$ ($\beta = 0.50$; b = 250 nm).
- High interface porosity, $\alpha_{pf\,(2)} = 0.067$ ($\beta = 1$; b = 250 nm).

An interface gap of 250 nm is considered to be a high, but still a realistic gap size. In the calculations, a diameter of 15 μm is used for the assumed circular glass fibers. The three other porosity factors ($\alpha_{pf\,(1)}$, $\alpha_{pf\,(3)}$, and $\alpha_{pm\,(1)}$) are set equal to zero, which means that the composites are considered to contain interface porosity only (in addition to structural porosity after the transition point). In Fig. 9, schematized cross-sections of composites with the three levels of interface porosity are shown.
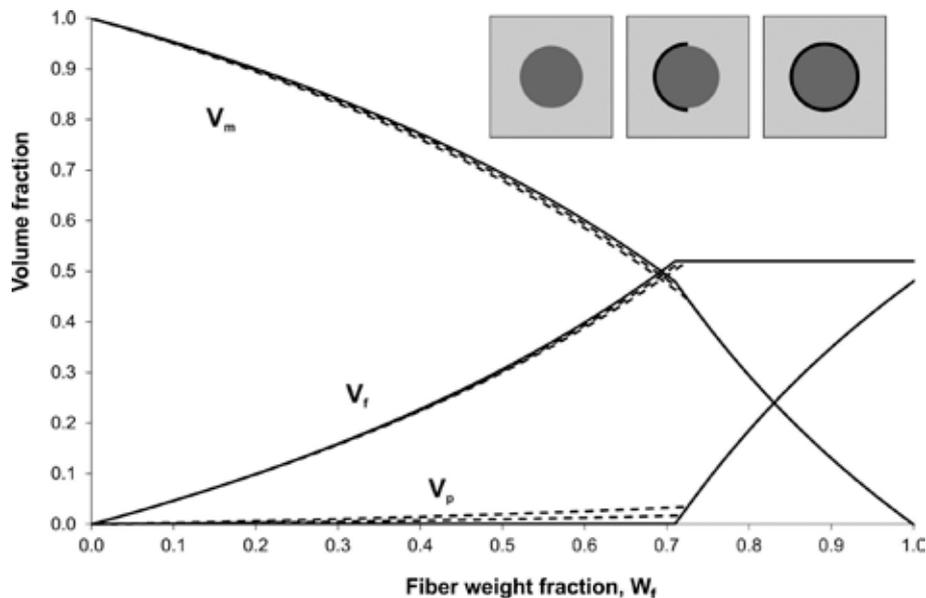

Fig. 9. Model predictions of the volumetric composition in glass fiber/epoxy composites with three levels of interface porosity. Solid lines show no porosity, and dotted lines show medium and high levels of porosity. Schematized cross-sections of the composites are shown. See more details in the text.

As can be observed in Fig. 9, the existence of interface porosity in composites has only a relatively small influence on the overall volumetric composition. Only for the case of the highest level of interface porosity where the interface gap is considered to exist along the entire fiber perimeter, the porosity of the composites is noticeable above zero (e.g. V_p is equal to 0.035 at the transition point), but still the curves for V_f and V_m are only slightly lowered.

50

Accordingly, as might have been expected, and is quantitatively confirmed by the model, the existence of interface porosity in composites will have a negligible effect on the volumetric composition (although it might have a large effect on the mechanical properties). Thus, the effect of changing the degree of fiber/matrix compatibility is not likely to be observed by changes of the volumetric composition in the composites.

4.3 Effect of air entrapment in matrix. The avoidance of entrapped air bubbles in the matrix is a well-known challenge in the processing of composites. The air bubbles are typically formed due to non-ideal process conditions. For thermoplastic matrix composites, entrapped air bubbles can be formed due to non-optimal settings (i.e. time, temperature, and pressure) of the melting, consolidation, solidifying processes. For thermosetting matrix composites, entrapped air bubbles can be formed due to (i) insufficient evacuation of the resin prior to fiber impregnation, (ii) inclusion of air in the resin during fiber impregnation, e.g. by roller actions in hand-layup methods, and by leakage in vacuum methods, and (iii) generation of volatile by-products, such as water, during curing of the resin.

The above presented model of volumetric composition contains parameters for quantifying the content of matrix porosity. In Eq. (18), the matrix porosity factor ($\alpha_{pm\,(1)}$) is related to the volume fraction of porosity in the matrix ($V_{matrix\,porosity}$) by a simple relationship containing only this parameter. A value for $V_{matrix\,porosity}$ can be determined by composite cross-sectional measurement of the content of air cavities in matrix-rich regions. Alternatively, a value for $V_{matrix\,porosity}$ can be determined by fitting the model to experimental data.

In the study by Domínguez and Madsen (2013), a series of biaxial glass fiber/polyfurfuryl alcohol (FA) resin composites was made by hand-layup followed by a double-vacuum bag technique. FA is a newly developed biomass-based resin (Pohl et al. 2011; Domínguez, Grivel and Madsen 2012). Water is used as solvent in the FA resin to lower the viscosity, and in addition, water is generated as by-product in the condensation reactions taking place during curing of the resin. Thus, specially adapted process conditions are required to ensure that water is removed (e.g. by evaporation) from the FA resin before it becomes trapped in the cured resin leading to air-filled cavities. The double-vacuum bag technique is specially developed for this purpose (Hou and Jensen 2008).

In the study by Domínguez and Madsen (2013), the series of glass/FA composites was made with variable amount of the impregnating FA resin. The volumetric composition in the composites was measured, and the experimental data is shown in Fig. 10. It can be seen that the composites contain a non-negligible content of porosity (V_p is in the range 0.03 to 0.08), which indicate that the process conditions can be furthermore optimized. However, it can be observed that the porosity tends to be decreased when the fiber content is increased, or expressed in another way, the porosity tends to be increased when the matrix content is increased. This tendency is interpreted as being a result of matrix porosity, which is known to be a special concern for the FA resin, as described above.

In Fig. 10, the volumetric composition model has been fitted to the experimental data of the glass/FA composites. The values of the model parameters are presented in Table 1. It is assumed that the composites contain only matrix porosity, i.e. there is no fiber porosity due to the massive nature of glass fibers, there is no interface porosity due to the high degree of compatibility between glass fibers and FA resin, and there is no impregnation porosity due to the low viscosity of the FA resin ensuring complete impregnation of the glass fiber bundles. Thus, $\alpha_{pf\,(1)}$, $\alpha_{pf\,(2)}$, and $\alpha_{pf\,(3)}$ are assumed to be equal to zero. Based on the fitted model lines in Fig. 10, the value of the matrix porosity factor, $\alpha_{pm\,(1)}$, is determined to be 0.10, leading to a value of $V_{matrix\,porosity}$ on 0.09 (Eq. (18)). Thus, in matrix-rich regions of the glass/FA

51

composites, the content of porosity is 0.09. In other words, a sample of neat FA resin (made by similar processing conditions) would have a porosity content of 0.09, which can be seen for the model line for V_p in Fig. 10 at $W_f = 0$ (and $V_f = 0$). This leads to a porosity content of the composites on 0.04 at the transition point.

In Fig. 10, model lines are also calculated for the case of glass/FA composites with no matrix porosity ($\alpha_{pm\ (1)} = 0$). It can be observed that the no porosity lines of V_f and V_m deviate considerably from the lines of the glass/FA composites with matrix porosity. Especially, it can be noted, as expected, that the (large) deviation between the lines for V_m is getting larger when the fiber content is decreased, whereas the (small) deviation between the lines for V_f is getter smaller. In a more practically applied context, however, the model lines in Fig. 10 for the glass/FA composites with no matrix porosity can be used to assess the potential improvement in volumetric composition (and thereby mechanical properties) of the manufactured composites if the processing conditions is furthermore optimized.

Altogether, it has been demonstrated that air entrapment in the matrix is likely to have a marked effect on the volumetric composition in the composites, and the model can be used as a tool for a quantitative analysis of the effect.
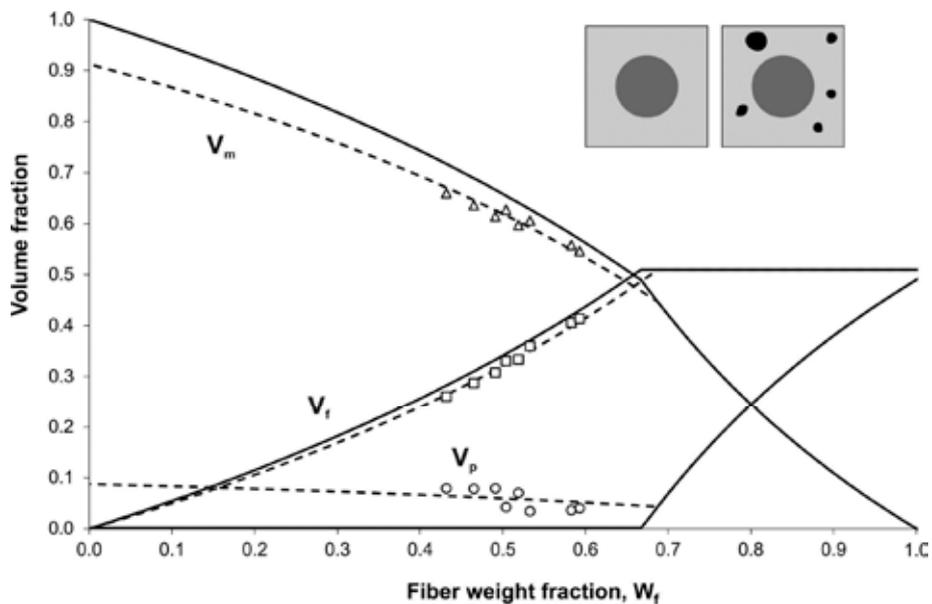

Fig. 10. Experimental data and model calculations of the volumetric composition in biaxial (± 45°) glass fiber/FA composites. Solid lines are predictions for composites with no porosity, and dotted lines are fitted to the experimental data for composites with matrix porosity. Schematized cross-sections of the composites are shown. See more details in the text.

5.   CONCLUSIONS AND FUTURE WORK

A model for the volumetric composition in composites is presented, where the volume fractions of fibers, matrix and porosity are calculated as a function of the fiber weight fraction. The model includes the realistic case of composites with porosity, and limited fiber packing ability. The porosity is addressed via a number of so-called porosity factors, which can be related to the composite microstructure. The limited packing ability of the fiber assembly is addressed via the so-called maximum obtainable fiber volume fraction, $V_{f\,max}$.

The model defines two regions of composite volumetric composition, Region A and B, separated by a transition fiber weight fraction, at which the composites show the best possible combination of high fiber volume fraction and low porosity leading to composites with the best possibly mechanical properties.

Based on experimental data of composites manufactured with different process conditions, together with model predictions, a quantitative analysis is presented for three types of process related effects on the volumetric composition in composites: (i) consolidation pressure, (ii) fiber/matrix compatibility, and (iii) air entrapment in matrix.

The applied consolidation pressure used in the manufacturing process is found to have a marked effect on the volumetric composition in composites. In general, the impregnation porosity is slightly decreased, and $V_{f\,max}$ is considerably increased, when the consolidation pressure is increased. As an example, for biaxial glass/epoxy composites manufactured by vacuum infusion, $V_{f\,max}$ is increased from 0.51 to 0.64 when the consolidation pressure is increased from 0.1 to 0.8 MPa. A power-law relationship, similar to the one commonly used to describe the compaction behavior of dry fiber assemblies, is found to well describe the relation between $V_{f\,max}$ in composites and the applied consolidation pressure.

The degree of fiber/matrix compatibility and the related amount of interface porosity is found to have a negligible effect on the volumetric composition. Only for the case of a very high level of interface porosity where an interface gap of 250 nm is considered to exist along the entire fiber perimeter, the porosity of the composites is noticeable above zero, but still the fiber and matrix volume fractions are only slightly changed. Thus, the effect of changing the degree of fiber/matrix compatibility is not likely to be observed by changes of the volumetric composition.

Air entrapment in the matrix due to non-ideal process conditions is found to have a marked effect on the volumetric composition in composites. For composites with such type of matrix porosity, the porosity content is decreased when the fiber content is increased. As an example, for biaxial glass/polyfurfuryl alcohol composites manufactured by a double vacuum bag technique, the porosity content in the matrix-rich regions is determined to be 0.09. This is then the porosity content of the neat resin at zero fiber content, leading to a porosity content of 0.04 for composites with a high fiber content at the transition point.

Altogether, it is demonstrated that the presented model of volumetric composition in composites is a valuable tool for a quantitative analysis of the effect of process conditions.

Based on the findings and considerations in the present study, examples of future work can be mentioned for the further improvement of the model:
- Development of analytical model for the content of impregnation porosity in composites. This important type of porosity is related to the configuration of the fiber assembly (e.g. fiber dispersion), in addition to the matrix flow behavior.
- Development of analytical model for the relationship between consolidation pressure and

$V_{f\,max}$ in composites. Important parameters are the configuration of the fiber assembly (e.g. fiber orientation and length), the fiber mechanical properties (e.g. stiffness), and the special conditions of the composite manufacturing process (e.g. matrix viscosity, lubrication, and creep).

REFERENCES

Aslan, M., Mehmood, S., and Madsen, B. (2013). Effect of consolidation pressure on volumetric composition and stiffness of unidirectional flax fibre composites. Journal of Materials Science. 48, 3812-3824.

Beil, N.B., and Roberts, W.W. (2002). Modeling and computer simulation of the compressional behaviour of fiber assemblies. Part I: Comparison to van Wyk's theory. Textile Research Journal. 72, 341-351.

Domínguez, J.C., Grivel, J.C., and Madsen, B. (2012). Study on the non-isothermal curing kinetics of a polyfurfuryl alcohol bioresin by DSC using different amounts of catalyst. Thermochimica Acta. 529, 29-35.

Domínguez, J.C., and Madsen, B. (2013). Optimization of the operating conditions used to produce new biomass-based composite materials by the double-vacuum bag technique. In preparation.

Gutowski, T.G., Cai, Z., Bauer, S., Boucher, D., Kingery, J., and Wineman, S. (1987). Consolidation experiments for laminate composites. Journal of Composite Materials. 21, 650-669.

Hou, T.H., and Jensen, B.J. (2008). Double-vacuum-bag technology for volatile management in composite fabrication. Polymer Composites. 29, 906-14.

Lomov, S.V., and Verpoest, I. (2000). Compression of woven reinforcements: A mathematical model. Journal of Reinforced Plastics and Composites. 19, 1329-1350.

Madsen B., Thygesen A., and Lilholt H. (2007). Plant fiber composites – porosity and volumetric interaction. Composites Science and Technology. 67: 1584-1600.

Madsen, B., and Lilholt, H. (2002). Compaction of plant fiber assemblies in relation to composite fabrication. In the Proceedings of the 23rd Risø International Symposium on Materials Science. Sustainable natural and polymeric composites – Science and technology. Risø National Laboratory, Roskilde, Denmark, p. 239-250.

Madsen, B., Thygesen, A., and Lilholt, H. (2009). Plant fibre composites – porosity and stiffness. Composites Science and Technology. 69, 1057-1069.

Markussen, C.M., Prabharakan, D.R.T., Toftegaard, H.L., and Madsen, B. (2013). Biobased hybrid composites for structural applications. In preparation.

Pohl, T., Bierer, M., Natter, E., Madsen, B., Hoydonckx, H., and Schledjewski, R. (2011). Properties of compression moulded new fully biobased thermoset composites with aligned flax textiles. Plastics, Rubber and Composites. 40, 294-299.

Simácek, P., and Karbhari, V.M. (1996). Notes on the modeling of preform compaction: I-Micromechanics at the fiber bundle level. Journal of Reinforced Plastics and Composites. 15, 86-122.

Toftegaard, H. (2002). Tensile testing of flax/PP laminates. Risø Report: Risø-I-1799(EN), Risø National Laboratory, Materials Research Department, Denmark. 92 pp.

Toll, S. (1998). Packing mechanics of fiber reinforcements. Polymer Engineering and Science. 38, 1337-1350.

Toll, S., and Manson, J.-A.E. (1995). Elastic compression of a fiber network. Journal of Applied Mechanics. 62, 233-236.